

# Stasis domains and slip surfaces in the locomotion of a bio-inspired two-segment crawler

PAOLO GIDONI<sup>1</sup> AND ANTONIO DESIMONE<sup>1,2,\*</sup>

<sup>1</sup>*SISSA – International School for Advanced Studies, via Bonomea 265, 34136 Trieste, Italy.*

<sup>2</sup>*GSSI – Gran Sasso Science Institute, viale Francesco Crispi 7, 67100 L'Aquila, Italy.*

## Abstract

We formulate and solve the locomotion problem for a bio-inspired crawler consisting of two active elastic segments (i.e., capable of changing their rest lengths), resting on three supports providing directional frictional interactions. The problem consists in finding the motion produced by a given, slow actuation history.

By focusing on the tensions in the elastic segments, we show that the evolution laws for the system are entirely analogous to the flow rules of elasto-plasticity. In particular, sliding of the supports and hence motion cannot occur when the tensions are in the interior of certain convex regions (stasis domains), while support sliding (and hence motion) can only take place when the tensions are on the boundary of such regions (slip surfaces).

We solve the locomotion problem explicitly in a few interesting examples. In particular, we show that, for a suitable range of the friction parameters, specific choices of the actuation strategy can lead to net displacements also in the direction of higher friction.

---

\*Corresponding author – e-mail address: [desimone@sissa.it](mailto:desimone@sissa.it) – phone: +39 040 3787 455

# 1 Introduction

Research on biological and bio-inspired locomotion, aimed at understanding and replicating motor abilities of animals capable of propelling effectively in environments where standard locomotion strategies fail (e.g., those based on wheels), is receiving increasing attention, starting from the seminal work by Hirose [8].

A promising area where interesting applications are envisaged is medical endoscopy, through the development of miniaturised biomedical robotic tools [9, 11]. Here, the need for non-standard bio-inspired solutions comes from size constraints (which make devices based on engine-powered shafts and cogwheels unfeasible) and from the challenge of extracting propulsive forces from the frictional interactions with soft biological tissues in a non-invasive way. Drawing inspiration from the locomotion strategies of worms (e.g., *Lumbricus terrestris*), and from the anchoring abilities of parasites and larvae, artificial bio-mimetic crawlers have been conceived, manufactured, and analysed. The system considered in [12], a prototypical example, consists of several elastic segments that can actively change their rest lengths (thanks to shape-memory-alloy wires, actuated with electric currents via Joule heating), and supported by hook-shaped elements that give a directional character to the frictional interactions with the environment (as in “hairy” surfaces, characterised by low friction when sliding occurs “along the grain”, and by high friction when sliding occurs in the opposite direction, “against the grain”). Similar systems have been investigated in the context of the more general robotics literature [2, 3, 21, 22], or in models for the propulsion of crawling cells [19]. In spite of the many interesting results contained in these studies, several open issues remain, even at the level of theoretical analysis. In particular, a detailed understanding of the general relation between actuation history, elastic tensions developed in the segments, and observable motions is still missing. In [12], for example, the simplifying assumption is made that motion in the high friction direction is forbidden, i.e., no back-sliding occurs. As a consequence, motion can only take place in one direction, the one of low resistance.

Inspired by these developments, and building upon previous work by our group [4, 5, 6, 7, 17, 18], we consider in this paper a model crawler lying on a horizontal surface, consisting of two linearly elastic segments that can actively change their rest length, and subject to horizontal frictional forces at their ends mimicking a directional frictional contact. We formulate the locomotion problem for this system in the regime of slow (quasi-static) actuation, in which inertial forces can be neglected, an actuation history is prescribed by assigning the time evolution of the rest length of the segments, and we

solve for the resulting motion. In this way, we extend the results obtained in [7], where the behaviour of a one-segment crawler was analysed. The increased complexity of the two segment crawler requires a methodological change. Indeed, we solve the problem by showing that the behaviour of the system is governed by the tensions arising in the elastic segments, and that the resulting laws of motion are entirely analogous to the flow rules typical of elasto-plasticity. In particular, there are convex domains in the plane of the internal tensions (stasis domains, the analog of elastic domains) corresponding to which no sliding of the supports can take place. Only when the tensions reach the boundaries of these domains (slip surfaces, the analog of yield surfaces), sliding of the supports, and hence motion of the segments can occur.

We solve the locomotion problem in a few interesting examples. In particular, we show that, for a suitable range of the friction parameters, specific choices of the actuation strategy can lead to net displacements also in the direction of higher friction. This last remark shows that, provided that the system is complex enough (i.e., it is made of at least two independent segments), it is not only motile (i.e., it can exhibit non-zero net displacements in at least one direction), but it is in fact controllable (it can move in both directions). It would be interesting to investigate whether a similar controllable motility scenario can also emerge in a different but related context, namely, forced brownian particles in a non-symmetric potential (forced thermal ratchets, see [10, 20]) which have been used as a model for the motion of motor proteins along microtubules and actin filaments.

The rest of the paper is organised as follows. In Section 2 we present our model of crawler and formulate the motility problem, introducing a necessary dimensional reduction that we discuss in detail in Section 3. In Section 4 we study the associated stasis domains and deduce the laws of motion, which are discussed in Section 5. Here, to better illustrate the situation, we construct and analyse two periodic motility strategies, generating displacement in opposite directions.

## 2 The crawler: formulation of the problem

We are interested in the motion of one-dimensional crawlers such as that represented in Figure 1. The crawler is composed of two adjacent rods, identified in the reference configuration by the segments  $[X_1, X_2]$  and  $[X_2, X_3]$ . We assume  $X_1 = 0$ ,  $X_2 = L_1$  and  $X_3 = L_1 + L_2$ , so that  $L_1$  and  $L_2$  are the reference lengths of the two rods. A point  $X$  of the crawler is mapped to the point  $x = \chi(X, t)$  in the deformed configuration and thus its displacement is

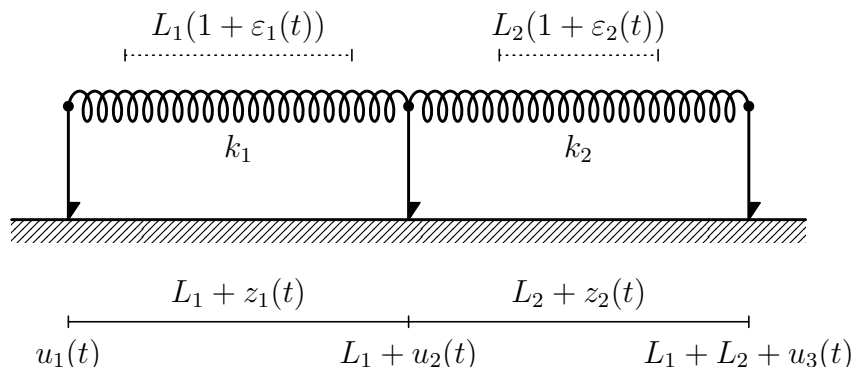


Figure 1: The model of our crawler. The dotted lines represent the rest lengths of the two springs.

$u(X, t) = \chi(X, t) - X$ . It is useful to set  $u_1(t) = u(X_1, t)$ ,  $u_2(t) = u(X_2, t)$  and  $u_3(t) = u(X_3, t)$ .

We denote the derivatives with respect to space and time with a prime and a dot, respectively,

$$u'(X, t) = \frac{\partial}{\partial X} u(X, t) \quad \dot{u}(X, t) = \frac{\partial}{\partial t} u(X, t) \quad (2.1)$$

The crawler interacts with the substrate only through three rigid legs located at  $X_1$ ,  $X_2$  and  $X_3$ . These interactions are described by the (directional) friction law

$$F_i(t) = F(X_i, t) \in \begin{cases} \{F_-\} & \text{if } \dot{u}_i(t) < 0 \\ [-F_+, F_-] & \text{if } \dot{u}_i(t) = 0 \\ \{-F_+\} & \text{if } \dot{u}_i(t) > 0 \end{cases} \quad (2.2)$$

where  $i = 1, 2, 3$ . We assume that

$$F_- > F_+ > 0 \quad (2.3)$$

This means that the absolute value of the friction force is not constant and depends on the direction of motion; moreover the coordinates are chosen so that negative velocities generate greater friction.

The two rods are assumed to be elastic, with stiffnesses  $k_1, k_2$ , and subject to an active distortion  $\varepsilon_0(X, t)$ . We assume that the distortion is uniform along each rod so that

$$\varepsilon_0(X, t) = \begin{cases} \varepsilon_1(t) & \text{if } X \in (0, L_1) \\ \varepsilon_2(t) & \text{if } X \in (L_1, L_1 + L_2) \end{cases} \quad (2.4)$$

The rest length of the two rods is thus  $(1 + \varepsilon_1(t))L_1$  and  $(1 + \varepsilon_2(t))L_2$ , respectively.

## 2.1 Internal energy and dissipation

For our analysis it is useful to describe the state of the crawler with two parameters  $z = (z_1, z_2)^t$  associated with its shape and a parameter  $y$  that identifies its position. More precisely, we set

$$z_1(t) = u_2(t) - u_1(t) \quad z_2(t) = u_3(t) - u_2(t) \quad y(t) = u_2(t) \quad (2.5)$$

As we will show, the internal energy of the crawler depends only on its shape and the dissipation, in almost all circumstances, can be expressed as a function of just the shape change  $\dot{z}$  through some minimality considerations. This will allow us to model the crawler as a rate independent dissipative system with quadratic (positive definite) energy, a situation well studied in elastoplasticity [13, 14].

The stored energy of the crawler is given by

$$\begin{aligned} \mathcal{E} &= \frac{k_1}{2} \int_0^{L_1} (u'(X, t) - \varepsilon_1)^2 dX + \frac{k_2}{2} \int_{L_1}^{L_1+L_2} (u'(X, t) - \varepsilon_2)^2 dX \\ &= \frac{k_1 L_1}{2} \left[ \frac{u_2(t) - u_1(t)}{L_1} - \varepsilon_1(t) \right]^2 + \frac{k_2 L_2}{2} \left[ \frac{u_3(t) - u_2(t)}{L_2} - \varepsilon_2(t) \right]^2 \\ &= \frac{1}{2} \langle Az(t), z(t) \rangle - \langle \ell(t), z(t) \rangle + c(t) \end{aligned} \quad (2.6)$$

where we have used the fact that minimal energy leads to  $X \mapsto u'(x, t)$  constant along each of the two rods, and we have set

$$\begin{aligned} A &= \begin{pmatrix} \frac{k_1}{L_1} & 0 \\ 0 & \frac{k_2}{L_2} \end{pmatrix} & \ell(t) &= \begin{pmatrix} k_1 \varepsilon_1(t) \\ k_2 \varepsilon_2(t) \end{pmatrix} \\ c(t) &= \frac{k_1 L_1 \varepsilon_1(t)^2}{2} + \frac{k_2 L_2 \varepsilon_2(t)^2}{2} \end{aligned}$$

We thus see that, for a prescribed active distortion  $\varepsilon(t)$ , the internal energy of the crawler depends only on time and on the shape  $z(t)$ , allowing us to write from now on  $\mathcal{E} = \mathcal{E}(t, z(t))$ .

The dissipation produced by the displacement  $u_i \mapsto u_i + v_i$  of a single contact point is

$$d(v_i) = v_i^+ F_+ - v_i^- F_- \quad (2.7)$$

where

$$v_i^+ = \begin{cases} v_i & \text{if } v_i \geq 0 \\ 0 & \text{if } v_i < 0 \end{cases} \quad \text{and} \quad v_i^- = \begin{cases} v_i & \text{if } v_i \leq 0 \\ 0 & \text{if } v_i > 0 \end{cases} \quad (2.8)$$

and therefore the dissipation produced by a shape change  $z \mapsto z + w$  and a position change  $y \mapsto y + v$  is

$$\mathcal{D}(w, v) = d(v - w_1) + d(v) + d(v + w_2) \quad (2.9)$$

We observe that  $\mathcal{D}$  is convex and positively homogeneous of degree 1.

For any fixed shape change  $w = \bar{w}$ , the function  $v \mapsto \mathcal{D}(\bar{w}, v)$  is convex and coercive, as it is the sum of convex and coercive functions of  $v$ . We now show that, under the additional hypothesis

$$F_- \neq 2F_+ \quad (2.10)$$

it has a unique minimum value, attained at  $v = v_{\min}(\bar{w})$ .

First of all we observe that  $\mathcal{D}(\bar{w}, \cdot)$  is differentiable everywhere except on the finite set  $\{\bar{w}_1, 0, -\bar{w}_2\}$ . The asymmetry of the friction (2.3) and the additional assumption (2.10) ensure that

$$\frac{\partial \mathcal{D}(\bar{w}, v)}{\partial v} \neq 0 \quad \text{for every } \bar{w} \in \mathbb{R}^2 \text{ and every } v \in \mathbb{R} \setminus \{\bar{w}_1, 0, -\bar{w}_2\} \quad (2.11)$$

Hence  $\mathcal{D}(\bar{w}, \cdot)$  has a unique minimum attained at  $v = v_{\min}(\bar{w}) \in \{\bar{w}_1, 0, -\bar{w}_2\}$ . With simple considerations on the sign of the derivative we can determine the exact value of  $v_{\min}$ . Precisely

$$v_{\min}(\bar{w}) = \begin{cases} \max\{\bar{w}_1, 0, -\bar{w}_2\} & \text{if } F_- > 2F_+ \\ \text{middle}(\bar{w}_1, 0, -\bar{w}_2) & \text{if } 2F_+ > F_- > F_+ \end{cases} \quad (2.12)$$

where we have introduced a ‘middle’ function that returns

- if its three arguments have all different values, the one with the middle value;
- if at least two arguments have the same value, that value.

More pragmatically, we order the triplet  $(\bar{w}_1, 0, -\bar{w}_2)$  and pick the middle element.

We observe that the  $v_{\min}$  is positively homogeneous of degree 1; its behaviour according to the values of the friction force is illustrated in Figure 2.

## 2.2 The variational inequality

We assume that the actuation history is slow enough (quasi-static) that inertial forces can be neglected. The evolution of the system is thus governed by the balance of forces, namely, by the fact that the sum of frictional resistance

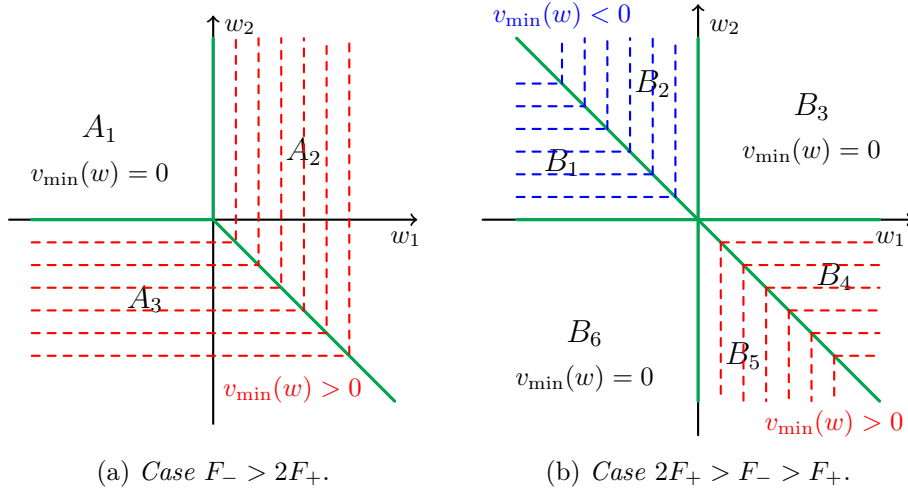


Figure 2: Contour plot (dashed) of the function  $v_{\min}(w)$  for different choices of the friction parameters.

forces  $F_i$  and elastic restoring forces is zero. This is expressed in abstract form by (SF) below and, more concretely, by the following three equations

$$\begin{cases} F_1 + \frac{k_1}{L_1}(z_1 - L_1\varepsilon_1) = 0 \\ F_2 - \frac{k_1}{L_1}(z_1 - L_1\varepsilon_1) + \frac{k_2}{L_2}(z_2 - L_2\varepsilon_2) = 0 \\ F_3 - \frac{k_2}{L_2}(z_2 - L_2\varepsilon_2) = 0 \end{cases} \quad (2.13)$$

An alternative way to write system (2.13) is to cast it in the form of a variational inequality (see [13, 15]). Doing this will enable us to exploit some known results on the evolution of rate independent systems. Therefore, we will write the laws governing the evolution of our system as a variational inequality first, and show later that this formulation leads to (SF) and (2.13).

For a given external load  $\ell(t)$ , the evolution  $z(t), y(t)$  of our system is obtained as a solution of the variational inequality

$$\langle Az(t) - \ell(t), w - \dot{z}(t) \rangle + \mathcal{D}(w, v) - \mathcal{D}(\dot{z}(t), \dot{y}(t)) \geq 0 \quad (\text{VI})$$

for every  $(w, v) \in \mathbb{R}^2 \times \mathbb{R}$ . In particular this must hold for  $w = \dot{z}(t)$ , for which we get

$$\mathcal{D}(\dot{z}(t), v) - \mathcal{D}(\dot{z}(t), \dot{y}(t)) \geq 0 \quad \text{for every } v \in \mathbb{R} \quad (2.14)$$

This is equivalent to set

$$\dot{y}(t) = v_{\min}(\dot{z}(t)) \quad (2.15)$$

We can use this fact to reduce the dimension of the problem associated to the variational inequality (VI), leading to

$$\langle Az(t) - \ell(t), w - \dot{z}(t) \rangle + \mathcal{D}_{\text{sh}}(w) - \mathcal{D}_{\text{sh}}(\dot{z}(t)) \geq 0 \quad \text{for every } w \in \mathbb{R}^2 \quad (\text{RVI})$$

where  $\mathcal{D}_{\text{sh}}$  is the ‘‘shape-restricted’’ dissipation, i.e. the dissipation after minimization with respect to translations of the crawler,

$$\mathcal{D}_{\text{sh}}(w) = \mathcal{D}(w, v_{\min}(w)) \quad (2.16)$$

This allows us to study the system for the shape changes alone and then recover the displacement  $y(t)$  of the crawler through the relationship (2.15).

Before discussing existence and uniqueness of the solutions for our problem, let us notice that  $\mathcal{D}_{\text{sh}}$  is convex (and therefore continuous) and positively homogeneous of degree 1. To show this, we recall that  $w \mapsto v_{\min}(w)$  is positively homogeneous of degree 1. Hence, for  $\lambda > 0$

$$\mathcal{D}_{\text{sh}}(\lambda w) = \mathcal{D}(\lambda w, v_{\min}(\lambda w)) = \mathcal{D}(\lambda w, \lambda v_{\min}(w)) = \lambda \mathcal{D}(w, v_{\min}(w)) = \lambda \mathcal{D}_{\text{sh}}(w)$$

Regarding the convexity of  $\mathcal{D}_{\text{sh}}$ , we observe that for every  $0 \leq \lambda \leq 1$ , writing  $w_\lambda = \lambda w + (1 - \lambda)\bar{w}$ , we have

$$\begin{aligned} \lambda \mathcal{D}_{\text{sh}}(w) + (1 - \lambda) \mathcal{D}_{\text{sh}}(\bar{w}) &\geq \lambda \mathcal{D}(w, v_{\min}(w)) + (1 - \lambda) \mathcal{D}(\bar{w}, v_{\min}(\bar{w})) \\ &\geq \mathcal{D}(w_\lambda, \lambda v_{\min}(w) + (1 - \lambda)v_{\min}(\bar{w})) \\ &\geq \mathcal{D}(w_\lambda, v_{\min}(w_\lambda)) = \mathcal{D}_{\text{sh}}(w_\lambda) \end{aligned} \quad (2.17)$$

Let us recall that the subdifferential of  $\mathcal{D}_{\text{sh}}$  in  $\bar{w}$  is defined as

$$\partial \mathcal{D}_{\text{sh}}(\bar{w}) = \{\xi \in \mathbb{R}^2 : \mathcal{D}_{\text{sh}}(w) \geq \mathcal{D}_{\text{sh}}(\bar{w}) + \langle \xi, w - \bar{w} \rangle \text{ for every } w \in \mathbb{R}^2\}$$

We remark that, strictly speaking, the subdifferential consists of elements of the dual space  $(\mathbb{R}^2)^*$ , but since we are working with finite dimensional spaces we implicitly adopt the usual identification of the elements of the dual with vectors of the space. Setting  $C^* = \partial \mathcal{D}_{\text{sh}}(0)$ , we observe that  $C^*$  is convex and satisfies

$$\mathcal{D}_{\text{sh}}(w) = \max_{\xi \in C^*} \langle \xi, w \rangle \quad (2.18)$$

We have the following result (cf. [14, Theorem 2.1]).

**Theorem 1.** *Given  $\ell \in \mathcal{C}^1([0, \mathcal{T}], \mathbb{R}^2)$  and  $z_0 \in A^{-1}(\ell(0) - C^*)$ , there exists a unique function  $z \in \mathcal{C}^{\text{Lip}}([0, \mathcal{T}], \mathbb{R}^2)$ , with  $z(0) = z_0$  and such that the shape-restricted variational inequality (RVI) is satisfied for almost all  $t \in [0, \mathcal{T}]$ .*

We remark that the dimensional reduction that allowed us to pass from  $\mathcal{D}$  to  $\mathcal{D}_{\text{sh}}$  is necessary to attain uniqueness, since the energy  $\mathcal{E}(t, \cdot)$  is not uniformly convex on  $\mathbb{R}^3$ , but becomes so if restricted to the shape coordinates  $z$ . When assumption (2.10) does not hold, it is possible to find multiple solutions for problem (VI), as shown by the following example.

Let us set  $F_- = 2F_+$  and assume that, at the initial time  $t = 0$ , the state of the crawler is such that both the springs are in the state of maximum compression, namely

$$\frac{k_1}{L_1}(z_1 - L_1\varepsilon_1) = -F_- \qquad \frac{k_2}{L_2}(z_2 - L_2\varepsilon_2) = -F_+$$

We consider an external load such that, for  $t \in [0, \mathcal{T}]$ , we have  $\dot{\varepsilon}_1(t) > 0$  and  $\dot{\varepsilon}_2(t) = 0$ . Under this conditions, the system has infinite solutions, identified by the parameter  $\mu \in [0, 1]$  and defined by

$$\dot{u}_1(t) = -\mu L_1 \dot{\varepsilon}_1(t) \qquad \dot{u}_2(t) = \dot{u}_3(t) = (1 - \mu)L_1 \dot{\varepsilon}_1(t)$$

We also observe that, using the definition of subdifferential, the variational inequality (RVI) can be restated as

$$0 \in \partial \mathcal{D}_{\text{sh}}(\dot{z}(t)) + D_z \mathcal{E}(t, z(t)) \qquad (\text{SF})$$

that is called the *subdifferential formulation* of the problem.

As remarked above, since inertial forces can be neglected in the regime of quasi-static actuation, (SF) is a force balance stating that the sum of dissipative frictional forces  $\partial \mathcal{D}_{\text{sh}}(\dot{z}(t))$  and elastic restoring forces  $D_z \mathcal{E}(t, z(t))$  must vanish at all times.

### 3 The shape-dependent dissipation

Our next step is therefore to study the restricted dissipation  $\mathcal{D}_{\text{sh}}$  and express more explicitly its differential. We consider separately the two cases  $F_- > 2F_+$  and  $2F_+ > F_- > F_+$ , since a different behaviour is observed.

#### 3.1 Case $F_- > 2F_+$

We divide the plane into three regions  $A_1$ ,  $A_2$  and  $A_3$ , as shown in Figure 3.

( $A_1$ ) This is the region defined by  $w_1 \leq 0 \leq w_2$ , that implies  $v_{\min}(w) = 0$  and

$$\mathcal{D}_{\text{sh}}(w) = (-w_1 + w_2)F_+ = \langle \alpha_1, w \rangle \qquad \text{where } \alpha_1 = \begin{pmatrix} -F_+ \\ F_+ \end{pmatrix}$$

(A<sub>2</sub>) Here we have  $w_1 \geq 0$  and  $-w_2 \leq w_1$ , so  $v_{\min}(w) = w_1$  and

$$\mathcal{D}_{\text{sh}}(w) = (2w_1 + w_2)F_+ = \langle \alpha_2, w \rangle \quad \text{where } \alpha_2 = \begin{pmatrix} 2F_+ \\ F_+ \end{pmatrix}$$

(A<sub>3</sub>) Here we have  $w_2 \leq 0$  and  $-w_2 \geq w_1$ , so  $v_{\min}(w) = -w_2$  and

$$\mathcal{D}_{\text{sh}}(w) = (-w_1 - 2w_2)F_+ = \langle \alpha_3, w \rangle \quad \text{where } \alpha_3 = \begin{pmatrix} -F_+ \\ -2F_+ \end{pmatrix}$$

The subdifferential of  $\mathcal{D}_{\text{sh}}$  in the origin is the convex hull generated by  $\alpha_1, \alpha_2, \alpha_3$  (cf. Fig. 5), namely

$$C_A^* = \partial \mathcal{D}_{\text{sh}}(0) = \text{conv}\{\alpha_1, \alpha_2, \alpha_3\} \quad (3.1)$$

If  $w \in \text{int } A_i$ , then  $\partial \mathcal{D}_{\text{sh}}(w) = \alpha_i$ , whereas if  $w \in A_i \cap A_j \setminus \{0\}$ , then  $\partial \mathcal{D}_{\text{sh}}(w) = \overline{\alpha_i \alpha_j}$ , where the latter denotes the edge of  $C_A^*$  having endpoints  $\alpha_i$  and  $\alpha_j$ , namely  $\overline{\alpha_i \alpha_j} = \text{conv}\{\alpha_i, \alpha_j\}$ .

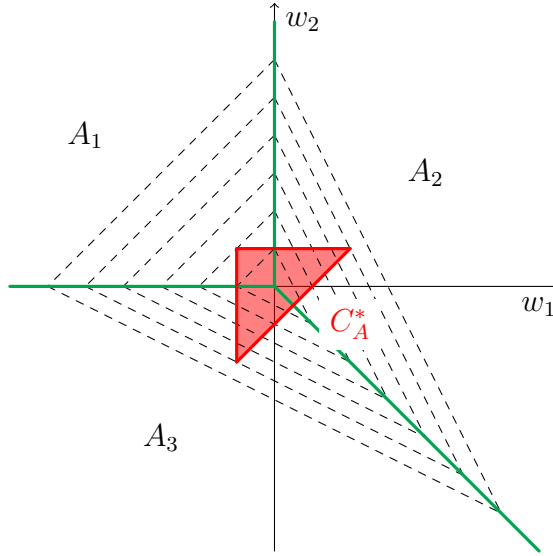


Figure 3: Case  $F_- > 2F_+$ . The three regions  $A_1, A_2$  and  $A_3$ , the contour lines of  $\mathcal{D}_{\text{sh}}$  (dashed) and its subdifferential at the origin  $C_A^*$  (red).

### 3.2 Case $2F_+ > F_- > F_+$

In this case we have to divide the plane into six different regions, as shown in Figure 4.

( $B_1$ ) Here  $w_1 \leq -w_2 \leq 0$  and so  $v_{\min}(w) = -w_2$ . In this region we have

$$\mathcal{D}_{\text{sh}}(w) = (-w_1 - w_2)F_+ + (w_2)F_- = \langle \beta_1, w \rangle \quad \text{where } \beta_1 = \begin{pmatrix} -F_+ \\ -F_+ + F_- \end{pmatrix}$$

( $B_2$ ) Here  $-w_2 \leq w_1 \leq 0$  holds, so  $v_{\min}(w) = w_1$ . In this region we have

$$\mathcal{D}_{\text{sh}}(w) = (w_1 + w_2)F_+ + (-w_1)F_- = \langle \beta_2, w \rangle \quad \text{where } \beta_2 = \begin{pmatrix} F_+ - F_- \\ F_+ \end{pmatrix}$$

( $B_3$ ) Here  $-w_2 \leq 0 \leq w_1$  holds, so  $v_{\min}(w) = 0$ . In this region we have

$$\mathcal{D}_{\text{sh}}(w) = (w_2)F_+ + (w_1)F_- = \langle \beta_3, w \rangle \quad \text{where } \beta_3 = \begin{pmatrix} F_- \\ F_+ \end{pmatrix}$$

( $B_4$ ) Here  $0 \leq -w_2 \leq w_1$  holds, so  $v_{\min}(w) = -w_2$ . In this region we have

$$\mathcal{D}_{\text{sh}}(w) = (-w_2)F_+ + (w_1 + w_2)F_- = \langle \beta_4, w \rangle \quad \text{where } \beta_4 = \begin{pmatrix} F_- \\ -F_+ + F_- \end{pmatrix}$$

( $B_5$ ) Here  $0 \leq w_1 \leq -w_2$  holds, so  $v_{\min}(w) = w_1$ . In this region we have

$$\mathcal{D}_{\text{sh}}(w) = (w_1)F_+ + (-w_1 - w_2)F_- = \langle \beta_5, w \rangle \quad \text{where } \beta_5 = \begin{pmatrix} F_+ - F_- \\ -F_- \end{pmatrix}$$

( $B_6$ ) Here  $w_1 \leq 0 \leq -w_2$  holds, so  $v_{\min}(w) = 0$ . In this region we have

$$\mathcal{D}_{\text{sh}}(w) = (-w_1)F_+ + (-w_2)F_- = \langle \beta_6, w \rangle \quad \text{where } \beta_6 = \begin{pmatrix} -F_+ \\ -F_- \end{pmatrix}$$

The subdifferential of  $\mathcal{D}_{\text{sh}}$  in the origin is

$$C_B^* = \partial\mathcal{D}_{\text{sh}}(0) = \text{conv}\{\beta_1, \beta_2, \beta_3, \beta_4, \beta_5, \beta_6\} \quad (3.2)$$

If  $w \in \text{int } B_i$ , then  $\partial\mathcal{D}_{\text{sh}}(w) = \beta_i$ , whereas if  $w \in B_i \cap B_j \setminus \{0\}$ , then  $\partial\mathcal{D}_{\text{sh}}(w) = \overline{\beta_i \beta_j}$ , using the notation we introduced in the previous case.

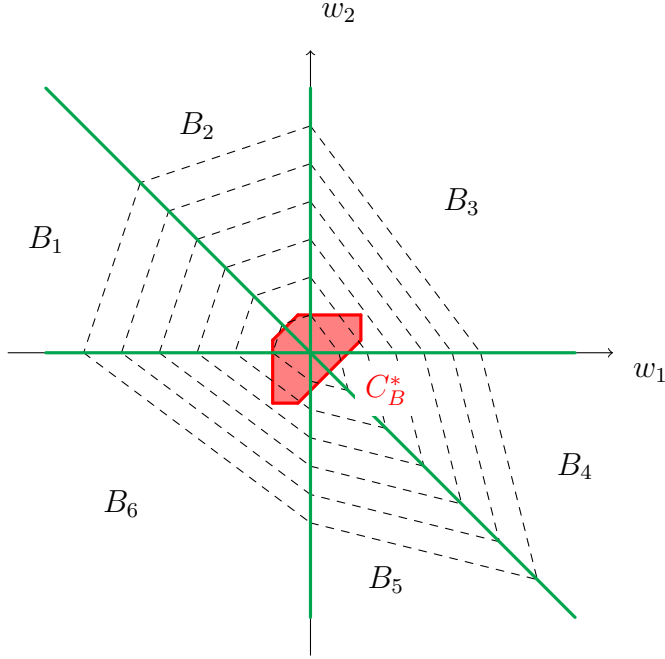


Figure 4: Case  $2F_+ > F_- > F_+$ . The six regions  $B_1, \dots, B_6$ , the contour lines of  $\mathcal{D}_{\text{sh}}$  (dashed) and its subdifferential at the origin  $C_B^*$  (red).

## 4 Stasis domains and the laws of motion

We observe that the gradient of  $\mathcal{E}$  with respect to the  $z$ -coordinates corresponds to the vector composed by the tensions of the two springs, i.e.

$$D_z \mathcal{E}(t, z(t)) = Az(t) - \ell(t) = \begin{pmatrix} \frac{k_1}{L_1} (z_1(t) - \varepsilon_1(t)L_1) \\ \frac{k_2}{L_2} (z_2(t) - \varepsilon_2(t)L_2) \end{pmatrix} = \begin{pmatrix} T_1(t) \\ T_2(t) \end{pmatrix} = T(t) \quad (4.1)$$

Thus, from (SF), we have

$$-T(t) \in \partial \mathcal{D}_{\text{sh}}(\dot{z}(t)) \quad (4.2)$$

We can distinguish between three different situations.

- If  $\dot{z}(t) = 0$ , then  $-T(t) \in C^*$ .
- If  $\dot{z}(t) \in \text{int } A_i$  for some  $i$ , then  $-T(t) = \alpha_i$ . Similarly, if  $\dot{z}(t) \in \text{int } B_i$  for some  $i$ , then  $-T(t) = \beta_i$ .

- If  $\dot{z}(t) \in A_i \cap A_j \setminus \{0\}$  for some  $i \neq j$ , then  $-T(t) \in \overline{\alpha_i \alpha_j}$ . Similarly, if  $\dot{z}(t) \in B_i \cap B_j \setminus \{0\}$  for some  $i \neq j$ , then  $-T(t) \in \overline{\beta_i \beta_j}$ .

This gives us a first description of the behaviour of our system. The tensions of the springs are allowed to change only within the set  $-C^*$ , that we call *stasis domain*, in analogy with the elastic domains used in elastoplasticity. Shape changes, and therefore motion, can occur only if the tensions have values on the boundary of  $-C^*$ , to which we refer as *slip surface*.

The next step is to use the information contained in (4.2), combined with the definition of  $T(t)$ , to recover how variations in the active distortion produce shape changes. The best way to do that is to work in terms of the tension state of the crawler  $T(t)$  instead of the shape state  $z(t)$ .

First of all we notice that, by differentiating (4.1), we get

$$\dot{T}_1(t) = -k_1 \dot{\varepsilon}_1(t) + \frac{k_1}{L_1} \dot{z}_1(t) \quad (4.3a)$$

$$\dot{T}_2(t) = -k_2 \dot{\varepsilon}_2(t) + \frac{k_2}{L_2} \dot{z}_2(t) \quad (4.3b)$$

If  $-T(t) \in \text{int } C^*$ , from (4.2) we have  $\dot{z}(t) = 0$  and the previous equations reduce to

$$\dot{T}_1(t) = -k_1 \dot{\varepsilon}_1(t) \quad \dot{T}_2(t) = -k_2 \dot{\varepsilon}_2(t) \quad (4.4)$$

that describe the evolution of the system. On the other end, when  $T(t)$  lies on the boundary of  $-C^*$ , the behaviour of the system is less trivial. We will discuss first the simpler case  $F_- > 2F_+$  and then consider the second case  $2F_+ > F_- > F_+$ .

#### 4.1 Case $F_- > 2F_+$

First of all let us introduce the unit vectors

$$\nu_1 = \frac{1}{\sqrt{2}} \begin{pmatrix} 1 \\ -1 \end{pmatrix} \quad \nu_2 = \begin{pmatrix} -1 \\ 0 \end{pmatrix} \quad \nu_3 = \begin{pmatrix} 0 \\ 1 \end{pmatrix}$$

that are the outer unit normals to  $C_A^*$  respectively along the edges  $\overline{\alpha_2 \alpha_3}$ ,  $\overline{\alpha_3 \alpha_1}$  and  $\overline{\alpha_1 \alpha_2}$ . The constraint  $-T(t) \in C_A^*$  implies that, if  $T$  is differentiable at time  $t$ , then

$$\begin{aligned} \langle \dot{T}(t), \nu_1 \rangle &= 0 & \text{if } -T(t) \in \overline{\alpha_2 \alpha_3} \\ \langle \dot{T}(t), \nu_2 \rangle &= 0 & \text{if } -T(t) \in \overline{\alpha_3 \alpha_1} \\ \langle \dot{T}(t), \nu_3 \rangle &= 0 & \text{if } -T(t) \in \overline{\alpha_1 \alpha_2} \end{aligned} \quad (4.5)$$

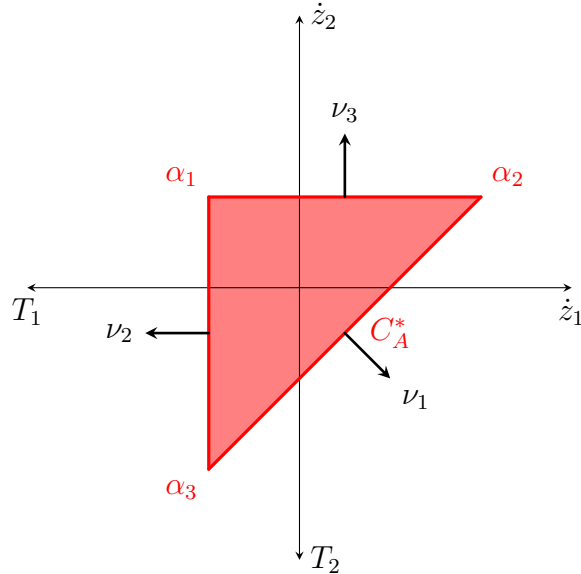


Figure 5: Case  $F_- > 2F_+$ . The stasis domain  $-C_A^* = -\partial\mathcal{D}_{\text{sh}}(0)$ .

If one of the scalar products were positive, then the tension should have been outside the stasis domain  $C_A^*$  for the times immediately before, and similarly, if one of them were negative, the tension would be outside  $C_A^*$  for the times immediately after.

Let us note that condition 4.5 can be expressed in a more concise way as

$$-T(t) \in N_{C_A^*}(T(t)) \quad (4.6)$$

where  $N_C(T)$  denotes the normal cone to the convex set  $C$  at the point  $T$ . This is also a classical way to approach the problem (RVI), usually known as *differential inclusion* formulation [13, 14].

Following this same line of thought, each of the constraints could be decoupled into two inequalities on the increments of  $T$ , one for the past and one for the future, without requiring the differentiability of  $T$ . However, for our purposes, we will work under the assumptions of Theorem 1, that guarantees the Lipschitz continuity of the tension  $T(t)$ , so that the times when  $T(t)$  is not differentiable can be neglected for the study of the motion.

A consequence of (4.5) is that, when we reach an edge, either the tension is differentiable, that implies  $\langle \dot{\ell}(t), \nu_i \rangle = 0$  and thus means that  $\varepsilon(t)$  is in

a certain sense “well calibrated”, or we have a time  $t$  of non-differentiability for  $T(t)$  and  $z(t)$ , corresponding to an abrupt transition between rest and motion.

If  $-T(t)$  lies on one on the vertices of  $C_A^*$ , then two of the constraints of (4.5) are satisfied simultaneously, leading to

$$\dot{z}_1(t) = L_1 \dot{\epsilon}_1(t) \qquad \dot{z}_2(t) = L_2 \dot{\epsilon}_2(t) \qquad (4.7)$$

We also recall that, by (4.2), we know that  $\dot{z}(t) \in A_i$ ; combining this with (4.7) we see that, to keep that tension configuration, the derivative of the active distortion must lie in a specific cone. In more detail, we have the following situation.

- If  $-T(t) = \alpha_1$ , then by (4.5) we have  $\dot{z}_1(t) \leq 0 \leq \dot{z}_2(t)$  (i.e.  $\dot{z}(t) \in A_1$ ), that implies  $\dot{v}(t) = 0$  and

$$\dot{\epsilon}_1(t) \leq 0 \leq \dot{\epsilon}_2(t)$$

The resulting motion of the crawler is

$$\dot{u}_1(t) = -L_1 \dot{\epsilon}_1(t) \geq 0 \qquad \dot{u}_2(t) = 0 \qquad \dot{u}_3(t) = L_2 \dot{\epsilon}_2(t) \geq 0$$

- If  $-T(t) = \alpha_2$ , then  $\dot{z}_1(t) \geq 0$  and  $\dot{z}_1(t) \geq -\dot{z}_2(t)$ , so that  $\dot{v}(t) = \dot{z}_1(t)$  and

$$\dot{\epsilon}_1(t) \geq 0 \qquad \text{and} \qquad \dot{\epsilon}_2(t) \geq -\frac{L_1}{L_2} \dot{\epsilon}_1(t)$$

The resulting motion of the crawler is

$$\begin{aligned} \dot{u}_1(t) &= 0 & \dot{u}_2(t) &= L_1 \dot{\epsilon}_1(t) \geq 0 \\ \dot{u}_3(t) &= L_1 \dot{\epsilon}_1(t) + L_2 \dot{\epsilon}_2(t) \geq 0 \end{aligned}$$

- If  $-T(t) = \alpha_3$ , then  $\dot{z}_2(t) \leq 0$  and  $\dot{z}_1(t) \leq -\dot{z}_2(t)$ , so that  $\dot{v}(t) = -\dot{z}_2(t)$  and

$$\dot{\epsilon}_2(t) \leq 0 \qquad \text{and} \qquad \dot{\epsilon}_1(t) \leq -\frac{L_2}{L_1} \dot{\epsilon}_2(t)$$

The resulting motion of the crawler is

$$\begin{aligned} \dot{u}_1(t) &= -L_1 \dot{\epsilon}_1(t) - L_2 \dot{\epsilon}_2(t) \geq 0 & \dot{u}_2(t) &= -L_2 \dot{\epsilon}_2(t) \geq 0 \\ \dot{u}_3(t) &= 0 \end{aligned}$$

If  $-T(t)$  lies in the interior of one on the edges of  $C_A^*$ , then condition (4.5) gives us only one constraint. However a second constraint is obtained by (4.2), since we know that, if  $-T(t) \in \text{int} \overline{\alpha_i \alpha_j}$ , then  $\dot{z}(t) \in A_i \cap A_j$ . In more detail, we have the following situation.

- If  $-T(t) \in \overline{\alpha_1\alpha_2}$  then we have  $\dot{v}(t) = 0$  and

$$\begin{aligned} \dot{z}_1(t) &= 0 & \dot{z}_2(t) &= L_2\dot{\varepsilon}_2(t) \geq 0 \\ \dot{T}_1(t) &= -k_1\dot{\varepsilon}_1(t) & \dot{T}_2(t) &= 0 \end{aligned}$$

The resulting motion of the crawler is

$$\dot{u}_1(t) = \dot{u}_2(t) = 0 \quad \dot{u}_3(t) = L_2\dot{\varepsilon}_2(t) \geq 0$$

- If  $-T(t) \in \overline{\alpha_3\alpha_1}$  then we have  $\dot{v}(t) = 0$  and

$$\begin{aligned} \dot{z}_1(t) &= -L_1\dot{\varepsilon}_1(t) \geq 0 & \dot{z}_2(t) &= 0 \\ \dot{T}_1(t) &= 0 & \dot{T}_2(t) &= -k_2\dot{\varepsilon}_2(t) \end{aligned}$$

The resulting motion of the crawler is

$$\dot{u}_1(t) = -L_1\dot{\varepsilon}_1(t) \geq 0 \quad \dot{u}_2(t) = \dot{u}_3(t) = 0$$

- If  $-T(t) \in \overline{\alpha_2\alpha_3}$ , differently from the two previous cases, we observe changes on the tension and length of both segments; however this happens in a coordinated fashion, namely,

$$\dot{z}_1(t) = -\dot{z}_2(t) = \dot{v}(t) = \frac{k_1\dot{\varepsilon}_1(t) - k_2\dot{\varepsilon}_2(t)}{\frac{k_1}{L_1} + \frac{k_2}{L_2}} \geq 0$$

that gives the condition  $\dot{\varepsilon}_1(t) \geq \frac{k_2}{k_1}\dot{\varepsilon}_2(t)$  for the admissible active distortion. The tension evolves according to

$$\dot{T}_1(t) = \dot{T}_2(t) = -\frac{L_1\dot{\varepsilon}_1(t) + L_2\dot{\varepsilon}_2(t)}{\frac{L_1}{k_1} + \frac{L_2}{k_2}}$$

The resulting motion of the crawler is

$$\dot{u}_1(t) = \dot{u}_3(t) = 0 \quad \dot{u}_2(t) = \frac{k_1\dot{\varepsilon}_1(t) - k_2\dot{\varepsilon}_2(t)}{\frac{k_1}{L_1} + \frac{k_2}{L_2}} \geq 0$$

## 4.2 Case $2F_+ > F_- > F_+$

As in the previous case, we want to exploit the constraint  $-T(t) \in C_B^*$  to deduce a condition on  $\dot{T}(t)$ . We observe that  $\underline{\nu}_1$ ,  $\underline{\nu}_2$  and  $\underline{\nu}_3$  are the outer unit normals respectively to the edges  $\overline{\beta_4\beta_5}$ ,  $\overline{\beta_6\beta_1}$  and  $\overline{\beta_2\beta_3}$ , but also the inner

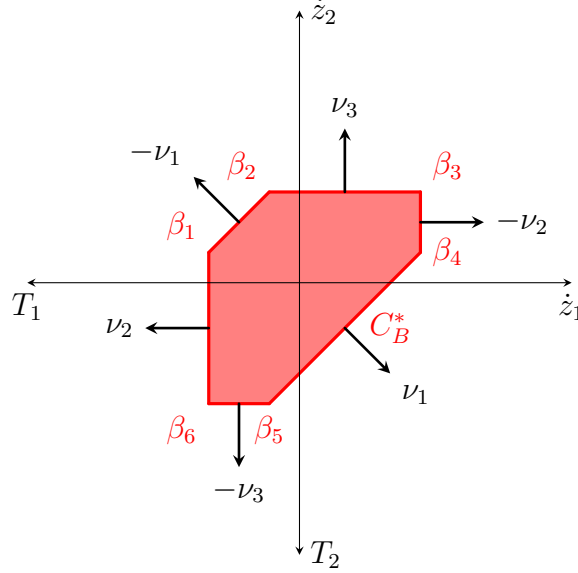


Figure 6: Case  $2F_+ > F_- > F_+$ . The stasis domain  $-C_B^* = -\partial\mathcal{D}_{\text{sh}}(0)$ .

unit normals to the edges  $\overline{\beta_1\beta_2}$ ,  $\overline{\beta_3\beta_4}$  and  $\overline{\beta_5\beta_6}$ . Thus we have, analogously to (4.5),

$$\begin{aligned}
\langle \dot{T}(t), \nu_1 \rangle &= 0 & \text{if } -T(t) \in \overline{\beta_4\beta_5} \cup \overline{\beta_1\beta_2} \\
\langle \dot{T}(t), \nu_2 \rangle &= 0 & \text{if } -T(t) \in \overline{\beta_6\beta_1} \cup \overline{\beta_3\beta_4} \\
\langle \dot{T}(t), \nu_3 \rangle &= 0 & \text{if } -T(t) \in \overline{\beta_2\beta_3} \cup \overline{\beta_5\beta_6}
\end{aligned} \tag{4.8}$$

As before, when  $-T(t)$  lies in one on the vertices of  $C_B^*$ , two of the constraints of (4.8) are satisfied simultaneously and therefore

$$\dot{z}_1(t) = L_1 \dot{\varepsilon}_1(t) \qquad \dot{z}_2(t) = L_2 \dot{\varepsilon}_2(t) \tag{4.9}$$

Similarly to the previous case, if  $-T(t) \in \beta_i$ , then by (4.2) we have  $\dot{z}(t) \in B_i$ , leading to the following situation.

- If  $-T(t) = \beta_1$ , then by (4.5) we have  $\dot{z}_1(t) \leq -\dot{z}_2(t) \leq 0$ , that implies  $\dot{v}(t) = -\dot{z}_2(t)$  and requires, when  $T(t)$  is differentiable, that

$$\dot{\varepsilon}_2(t) \geq 0 \qquad \dot{\varepsilon}_1(t) \leq -\frac{L_2}{L_1} \dot{\varepsilon}_2(t)$$

The resulting motion of the crawler is

$$\dot{u}_1(t) = -L_1\dot{\epsilon}_1(t) - L_2\dot{\epsilon}_2(t) \geq 0 \quad \dot{u}_2(t) = -L_2\dot{\epsilon}_2(t) \leq 0 \quad \dot{u}_3(t) = 0$$

- If  $-T(t) = \beta_2$ , then we have  $-\dot{z}_2(t) \leq \dot{z}_1(t) \leq 0$ , so that  $\dot{v}(t) = \dot{z}_1(t)$  and

$$\dot{\epsilon}_1(t) \leq 0 \quad \dot{\epsilon}_2(t) \geq -\frac{L_1}{L_2}\dot{\epsilon}_1(t)$$

The resulting motion of the crawler is

$$\dot{u}_1(t) = 0 \quad \dot{u}_2(t) = L_1\dot{\epsilon}_1(t) \leq 0 \quad \dot{u}_3(t) = L_1\dot{\epsilon}_1(t) + L_2\dot{\epsilon}_2(t) \geq 0$$

- If  $-T(t) = \beta_3$ , then we have  $\dot{z}_1(t) \geq 0$  and  $\dot{z}_2(t) \geq 0$ , so that  $\dot{v}(t) = 0$  and

$$\dot{\epsilon}_1(t) \geq 0 \quad \dot{\epsilon}_2(t) \geq 0$$

The resulting motion of the crawler is

$$\dot{u}_1(t) = -L_1\dot{\epsilon}_1(t) \leq 0 \quad \dot{u}_2(t) = 0 \quad \dot{u}_3(t) = L_2\dot{\epsilon}_2(t) \geq 0$$

- If  $-T(t) = \beta_4$ , then by (4.5) we have  $\dot{z}_1(t) \geq -\dot{z}_2(t) \geq 0$ , so that  $\dot{v}(t) = -\dot{z}_2(t)$  and

$$\dot{\epsilon}_2(t) \leq 0 \quad \dot{\epsilon}_1(t) \geq -\frac{L_2}{L_1}\dot{\epsilon}_2(t)$$

The resulting motion of the crawler is

$$\dot{u}_1(t) = -L_1\dot{\epsilon}_1(t) - L_2\dot{\epsilon}_2(t) \leq 0 \quad \dot{u}_2(t) = -L_2\dot{\epsilon}_2(t) \geq 0 \quad \dot{u}_3(t) = 0$$

- If  $-T(t) = \beta_5$ , then we have  $-\dot{z}_2(t) \geq \dot{z}_1(t) \geq 0$ , so that  $\dot{v}(t) = \dot{z}_1(t)$  and

$$\dot{\epsilon}_1(t) \geq 0 \quad \dot{\epsilon}_2(t) \leq -\frac{L_1}{L_2}\dot{\epsilon}_1(t)$$

The resulting motion of the crawler is

$$\dot{u}_1(t) = 0 \quad \dot{u}_2(t) = L_1\dot{\epsilon}_1(t) \geq 0 \quad \dot{u}_3(t) = L_1\dot{\epsilon}_1(t) + L_2\dot{\epsilon}_2(t) \leq 0$$

- If  $-T(t) = \beta_6$ , then we have  $\dot{z}_1(t) \leq 0$  and  $\dot{z}_2(t) \leq 0$ , so that  $\dot{v}(t) = 0$  and

$$\dot{\varepsilon}_1(t) \leq 0 \qquad \dot{\varepsilon}_2(t) \leq 0$$

The resulting motion of the crawler is

$$\dot{u}_1(t) = -L_1\dot{\varepsilon}_1(t) \geq 0 \qquad \dot{u}_2(t) = 0 \qquad \dot{u}_3(t) = L_2\dot{\varepsilon}_2(t) \leq 0$$

As in the previous case, when  $-T(t)$  lies in the interior of one on the edges of  $C_B^*$ , only one constraint is given by condition (4.8), but a second one is recovered by (4.2), using the fact that if  $-T(t) \in \text{int } \overline{\beta_i\beta_j}$ , then  $\dot{z}(t) \in B_i \cap B_j$ . The pairs of opposite edges are characterized by the same behaviour of the crawler, but associated with shape variations of opposite sign. In more detail, we have the following situation.

- If  $-T(t) \in \overline{\beta_2\beta_3} \cup \overline{\beta_5\beta_6}$  then we have  $\dot{v}(t) = 0$  and

$$\begin{aligned} \dot{z}_1(t) &= 0 & \dot{z}_2(t) &= L_2\dot{\varepsilon}_2(t) \\ \dot{T}_1(t) &= -k_1\dot{\varepsilon}_1(t) & \dot{T}_2(t) &= 0 \end{aligned}$$

so that it is required that  $\varepsilon_2(t) \geq 0$  if  $-T(t) \in \overline{\beta_2\beta_3}$ , whereas  $\varepsilon_2(t) \leq 0$  if  $-T(t) \in \overline{\beta_5\beta_6}$ . The resulting motion of the crawler is

$$\dot{u}_1(t) = \dot{u}_2(t) = 0 \qquad \dot{u}_3(t) = L_2\dot{\varepsilon}_2(t) \begin{cases} \geq 0 & \text{if } -T(t) \in \overline{\beta_2\beta_3} \\ \leq 0 & \text{if } -T(t) \in \overline{\beta_5\beta_6} \end{cases}$$

- If  $-T(t) \in \overline{\beta_3\beta_4} \cup \overline{\beta_6\beta_1}$  then we have  $\dot{v}(t) = 0$  and

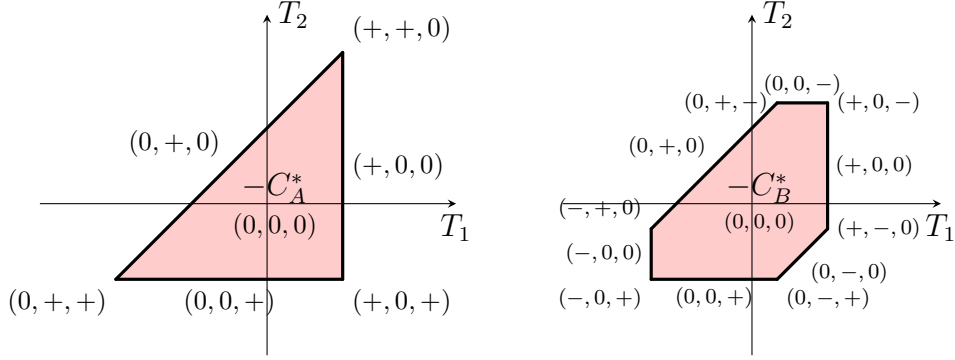
$$\begin{aligned} \dot{z}_1(t) &= -L_1\dot{\varepsilon}_1(t) & \dot{z}_2(t) &= 0 \\ \dot{T}_1(t) &= 0 & \dot{T}_2(t) &= -k_2\dot{\varepsilon}_2(t) \end{aligned}$$

so that it is required that  $\varepsilon_2(t) \geq 0$  if  $-T(t) \in \overline{\beta_6\beta_1}$ , whereas  $\varepsilon_2(t) \leq 0$  if  $-T(t) \in \overline{\beta_3\beta_4}$ . The resulting motion of the crawler is

$$\dot{u}_2(t) = \dot{u}_3(t) = 0 \qquad \dot{u}_1(t) = -L_1\dot{\varepsilon}_1(t) \begin{cases} \geq 0 & \text{if } -T(t) \in \overline{\beta_6\beta_1} \\ \leq 0 & \text{if } -T(t) \in \overline{\beta_3\beta_4} \end{cases}$$

- The third case  $-T(t) \in \overline{\beta_1\beta_2} \cup \overline{\beta_4\beta_5}$ , is characterized by a coordinated change in the tension and length of both segments, more precisely

$$\dot{z}_1(t) = -\dot{z}_2(t) = \dot{v}(t) = \frac{k_1\dot{\varepsilon}_1(t) - k_2\dot{\varepsilon}_2(t)}{\frac{k_1}{L_1} + \frac{k_2}{L_2}}$$



(a) Case  $F_- > 2F_+$ .

(b) Case  $2F_+ > F_- > F_+$ .

Figure 7: Qualitative summary of the motility results of section 4. Each triple is placed in the interior, on an edge or on a vertex of the stasis domain  $-C^*$  and describes the admissible directions of displacement for the three legs while the crawler keeps that tension configuration. A plus denotes a positive displacement, a minus a negative one and a zero that that leg must remain steady. For instance the triple  $(+, 0, -)$  near a vertex indicates that, for that value of the tension  $T(t)$ , we have  $\dot{u}_1(t) \geq 0$ ,  $\dot{u}_2(t) = 0$  and  $\dot{u}_3(t) \leq 0$ .

that gives, for the admissible active distortion, the condition  $\dot{\epsilon}_1(t) \geq \frac{k_2}{k_1} \dot{\epsilon}_2(t)$  if  $-T(t) \in \overline{\beta_4 \beta_5}$  and  $\dot{\epsilon}_1(t) \leq \frac{k_2}{k_1} \dot{\epsilon}_2(t)$  if  $-T(t) \in \overline{\beta_1 \beta_2}$ . The tension configuration evolves according to

$$\dot{T}_1(t) = \dot{T}_2(t) = -\frac{L_1 \dot{\epsilon}_1(t) + L_2 \dot{\epsilon}_2(t)}{\frac{L_1}{k_1} + \frac{L_2}{k_2}}$$

The resulting motion of the crawler is

$$\dot{u}_1(t) = \dot{u}_3(t) = 0 \quad \dot{u}_2(t) = \frac{k_1 \dot{\epsilon}_1(t) - k_2 \dot{\epsilon}_2(t)}{\frac{k_1}{L_1} + \frac{k_2}{L_2}} \begin{cases} \geq 0 & \text{if } -T(t) \in \overline{\beta_4 \beta_5} \\ \leq 0 & \text{if } -T(t) \in \overline{\beta_1 \beta_2} \end{cases}$$

## 5 Motility analysis and crawling strategies

A qualitative description of the results of the previous section is illustrated in Figure 7. The two possibilities considered for the relative magnitude of the friction forces determine very different motile behaviours of the crawler.

If  $F_- > 2F_+$ , the legs of the crawler can move only forward. The set  $-C_A^*$

of the admissible tension configurations scales with  $F_+$ , but it is independent of the value of  $F_-$ .

If  $2F_+ > F_- > F_+$ , each leg of the crawler can move both forward and backward. The precise shape of the stasis domain  $-C_B^*$  depends on the ratio  $F_+/F_-$ , although it is always a hexagon with parallel opposite edges oriented as in Figure 6. If the ratio  $F_+/F_-$  is fixed, then  $-C_B^*$  scales homothetically with the magnitude of the friction coefficients; if instead we fix the value of  $F_+$ , then  $-C_B^*$  shrinks as  $F_-$  tends to  $F_+$ .

To truly understand the motility of our crawler, we have to consider the effects of a periodic active distortion  $\varepsilon(t)$ . As a corollary of Theorem 1, we are granted the existence of a unique Lipschitz continuous displacement  $u(X, t)$  for any given continuous and piecewise continuously differentiable active distortion  $\varepsilon: [0, \mathcal{T}] \rightarrow \mathbb{R}^2$ .

We now discuss the main qualitative behaviour of such motility strategies and then present some illustrative examples. To simplify the computation, we assume  $k_1 = k_2 = k$  and  $L_1 = L_2 = L$ .

To produce a non-null translation of the crawler that repeats itself in each period, sufficiently large excursions in the stasis domain are necessary. More precisely, during every period the tension  $T(t)$  has to reach all the three edges of  $-C_A^*$  (if  $F_- > 2F_+$ ) or a suitable triple of non adjacent edges of  $-C_B^*$  (if  $2F_+ > F_- > F_+$ ). Since a certain amount of excursion in the active distortion is spent in crossing  $-C^*$ , allowing larger fluctuations in  $\varepsilon(t)$  permits more performant motility strategies, because in this way a larger amount of the active distortion is spent moving the legs.

In the case  $F_- > 2F_+$ , an effective motility strategy can be achieved even by activating only one of the segments, for instance by setting  $\varepsilon_2 \equiv 0$  and assuming a sufficiently large sawtooth oscillation for  $\varepsilon_1$ . This strategy can be compared to a one-segment crawler experiencing the same sawtooth fluctuations, as that studied in [6, Sec. 4]. Indeed, the one-segment crawler results more efficient: it requires a lower minimal amplitude  $\Delta\varepsilon$  of the sawtooth ( $\Delta\varepsilon > 2F_+/k$  instead of  $\Delta\varepsilon > 3F_+/k$ ), it produces a greater displacement after one cycle ( $\Delta u = (\Delta\varepsilon - 2F_+/k)L$  instead of  $\Delta u = (\Delta\varepsilon - 3F_+/k)L$ ) and it is effective also in the case  $2F_+ > F_- > F_+$ . For such friction ratios a two-segment crawler, performing the sawtooth strategy above, has a zero net displacement after one cycle.

We remark that in all the situations above, net displacements are possible only in the direction of lower friction. To achieve a *complete motility*, i.e. to be able to move also backwards (against the higher friction) using periodic shape changes, we need to consider the case  $2F_+ > F_- > F_+$  and strategies that fully exploit two shape parameters. This minimality of two

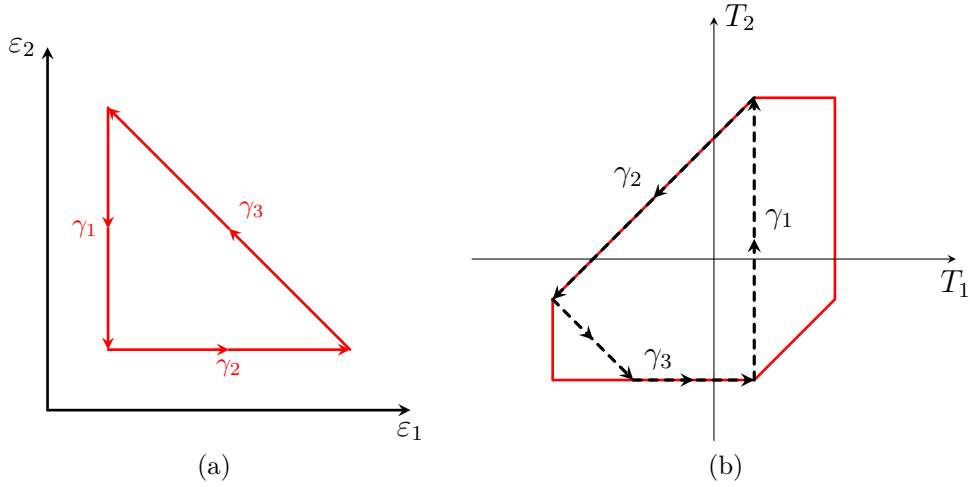


Figure 8: Active distortion strategy (5.1) and associated evolution of the tension.

shape parameters for a complete motility belongs to folklore knowledge for unidimensional locomotors (cf. for instance [1, 4, 7, 16]). The ability of our two-segment crawler to effectively move in both directions, assuming a small friction asymmetry, is illustrated by the following strategies.

We consider the periodic change in the active distortion illustrated in Figure 8, recalling that  $2F_+ > F_- > F_+$ . We set the times so that the period is  $\mathcal{T} = 3\tau$  and divide the evolution of  $\varepsilon(t)$  into three phases, described as follows.

$$\dot{\varepsilon}_1(t) = \begin{cases} 0 & \text{if } 0 < t < \tau \\ \eta & \text{if } \tau < t < 2\tau \\ -\eta & \text{if } 2\tau < t < 3\tau \end{cases} \quad \dot{\varepsilon}_2(t) = \begin{cases} -\eta & \text{if } 0 < t < \tau \\ 0 & \text{if } \tau < t < 2\tau \\ \eta & \text{if } 2\tau < t < 3\tau \end{cases} \quad (5.1)$$

where  $\eta > 0$  is a given parameter. We require that  $\eta\tau k > F_+ + F_-$ , to ensure sufficiently large distortions. Note that, since our system is rate independent, what really affects the resulting displacement is not  $\eta$  but the increment  $\eta\tau$  of the active distortion; actually, any other smooth time reparametrization of the curve in Figure 8 (a) would produce exactly the same displacement after each period.

The behaviour of the system in the first period depends on the initial state; however after the first period we always reach the same tension configuration  $T(3\tau) = -\beta_2$ . Since we are interested in the long term behaviour, we assume  $T(0) = -\beta_2$  and so avoid the initial adjustment period.

We now describe the behaviour in the three phases (see Fig. 8).

- ( $\gamma_1$ ) For  $0 < t < \frac{F_+ + F_-}{\eta k}$  the three legs are steady and  $T_2$  increases from  $-F_+$  to  $F_-$ . Then, for  $\frac{F_+ + F_-}{\eta k} < t < \tau$  the tension are constant but the third leg moves backwards with  $\dot{u}_3(t) = -\eta L$ .
- ( $\gamma_2$ ) For  $\tau < t < \frac{4F_- - 2F_+}{\eta k}$  the tension evolves from  $-\beta_5$  to  $-\beta_4$  along the corresponding edge of  $-C_B^*$ . At the same time, the middle leg moves forward with  $\dot{u}_2(t) = -\frac{\eta L}{2}$ . Once the tension edge  $-\beta_4$  is reached, for  $\frac{4F_- - 2F_+}{\eta k} < t < 2\tau$  the tension is constant, the middle leg is again steady while the first leg moves backwards with  $\dot{u}_1(t) = -\eta L$ .
- ( $\gamma_3$ ) For  $2\tau < t < \frac{2F_+ - F_-}{k}$ ,  $T_1$  increases and  $T_2$  decreases at the same rate, until they reach the edge of  $-C_B^*$ . Then, for  $\frac{2F_+ - F_-}{k} < t < \frac{3F_- - 3F_+}{k}$  the tension evolves along the edge until it reaches the vertex  $-\beta_2$ . In this time interval the third leg advances with  $\dot{u}_3(t) = L\eta$ . Finally, in the last interval  $\frac{3F_- - 3F_+}{k} < t < 3\tau$ , the tension is constant, the third leg is again steady and the middle leg moves backwards with  $\dot{u}_2(t) = -L\eta$ .

The sum of these actions produces in a period the displacement

$$\Delta^- u = L \left( \eta \mathcal{T} - \frac{4F_- - 2F_+}{k} \right) \quad (5.2)$$

We notice that the strategy we just presented could be slightly improved by suitably modifying  $\varepsilon(t)$ , for instance in a way to avoid the temporary forward movement of two of the legs. However these changes require an a priori knowledge of all the parameters of the systems, so that the strategy is, in a certain sense, calibrated to the situation, for instance requiring changes in  $\dot{\varepsilon}(t)$  exactly at the moment when the tension reaches the slip surface, i.e. the boundary of  $-C_B^*$ . The strategy we presented instead shows the same behaviour for every choice of the parameters, provided that the assumption of large distortions is satisfied. Moreover we remark that such improvements of the strategy decrease only the numerator of the negative term inside the brackets in (5.2), so the main term is untouched and any improvement becomes negligible for large distortions  $\eta \mathcal{T}$  or large stiffness  $k$ .

The history of active distortion (5.1) was also chosen to show a backward movement of the crawler, that corresponds to proceeding in the direction of higher friction. A simple strategy to move forwards is given by the time reverse of strategy (5.1), namely

$$\dot{\varepsilon}_1(t) = \begin{cases} \eta & \text{if } 0 < t < \tau \\ -\eta & \text{if } \tau < t < 2\tau \\ 0 & \text{if } 2\tau < t < 3\tau \end{cases} \quad \dot{\varepsilon}_2(t) = \begin{cases} -\eta & \text{if } 0 < t < \tau \\ 0 & \text{if } \tau < t < 2\tau \\ \eta & \text{if } 2\tau < t < 3\tau \end{cases} \quad (5.3)$$

Also in this case, after a preliminary stage, the tension configuration at the beginning of each period stabilizes to  $T = -\beta_2$ , that will be the starting condition in our analysis. The evolution of the tension is shown in Figure 9. After a period the displacement produced is

$$\Delta^+u = L \left( \eta\mathcal{T} - \frac{5F_+ - F_-}{2k} \right) \quad (5.4)$$

We have that

$$\Delta^+u - \Delta^-u = \frac{9}{2}L(F_- - F_+) > 0 \quad (5.5)$$

and so there is an advantage when moving in the direction of lower friction. This advantage becomes null as the ratio  $F_+/F_-$  tends to one, while it increases to a constant when we approximate the threshold case  $F_+/F_- = 2$ .

We notice that the difference  $\Delta^+u - \Delta^-u$  between the displacement produced by our twin strategies does not depend on the amplitude  $\eta\mathcal{T}$  of the distortion. This means that, if the crawler can produce only small distortions, but slightly greater than the lower threshold  $(F_+ + F_-)/k$ , then a very large number of iterations of the first strategy is necessary to obtain a negative displacement equal to the positive one produced by a cycle of the second strategy. On the other hand, if the crawler can produce very large distortions (i.e.  $\eta\mathcal{T} \rightarrow \infty$ ) the outcomes of the two strategies become comparable, in the sense that the ratio  $\Delta^+u/\Delta^-u$  tends to one.

We remark that reversing the strategy does not always reverse also the direction of motion, as it happens in the example above. A counterexample is given by the simple strategy

$$\dot{\epsilon}_1(t) = \begin{cases} \eta & \text{if } 0 < t < \tau \\ 0 & \text{if } \tau < t < 2\tau \\ -\eta & \text{if } 2\tau < t < 3\tau \end{cases} \quad \dot{\epsilon}_2(t) = \begin{cases} 0 & \text{if } 0 < t < \tau \\ \eta & \text{if } \tau < t < 2\tau \\ -\eta & \text{if } 2\tau < t < 3\tau \end{cases} \quad (5.6)$$

and its time-reverse, for sufficiently large distortions, namely  $\eta\mathcal{T} > 3F_-k$ . Both strategy (5.6) and its reverse produce the same, positive displacement after a period, equal to

$$\Delta u = L \frac{2F_- - F_+}{k} \quad (5.7)$$

We notice that in this case the displacement is independent of the distortion  $\eta\mathcal{T}$ , while with the previous strategies we had an asymptotically linear growth in terms of  $\eta\mathcal{T}$ . The inefficiency of this strategies with respect to (5.3) can be seen intuitively also by looking at the behaviour of the crawler during a cycle. The first and the third legs perform both a forward and a backward movement, of amplitude growing with  $\eta\mathcal{T}$ , that almost cancel each other out, leaving only the final displacement  $\Delta u$ .

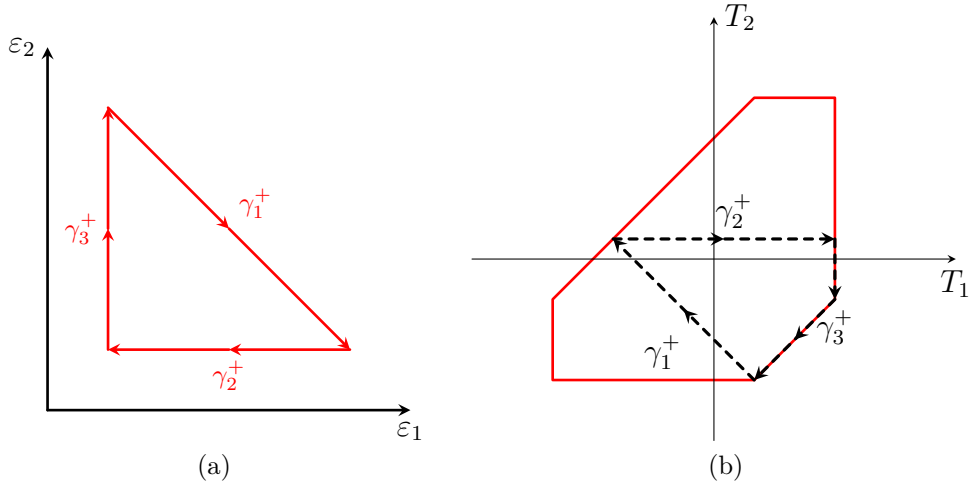


Figure 9: Active distortion strategy (5.3) and associated evolution of the tension.

We conclude by remarking that the approach adopted in this paper can be extended also to analogous crawlers composed by a larger number of segments. Increasing the number of legs enlarges the range of friction ratios under which motility in both directions is possible from  $F_+ < F_- < 2F_+$  to  $F_+ < F_- < NF_+$ . Intuitively, a  $N$ -segment crawler can move each leg backwards one by one, by leaning against the other  $N - 1$  legs, resulting in a strategy that generalizes (5.1). However the number of different scenarios that appear by varying the friction ratio also increases with the number of segments, and a complete and detailed description of a generic evolution problem becomes soon burdensome.

## Acknowledgement

This work has been supported by the ERC Advanced Grant 340685-MicroMotility.

## References

- [1] Arroyo, M., Heltai, L., Milan, D., DeSimone, A. 2012. Reverse engineering the euglenoid movement. Proc. Nat. Acad. Sci. USA 109: 17874-17879. (doi: 10.1073/pnas.1213977109)
- [2] Bolotnik, N., Pivovarov, M., Zeidis, I. and Zimmermann, K. 2015. On the motion of lumped-mass and distributed-mass self-propelling

- systems in a linear resistive environment. *Z. angew. Math. Mech.*. (doi: 10.1002/zamm.201500091)
- [3] Borisenko, I.N., Figurina, T.Yu., Chernousko, F.L., 2014. The quasi-static motion of a three body system on a plane, *J. Appl. Math. Mech.* 78, 220-227. (doi: 10.1016/j.jappmathmech.2014.09.003)
- [4] DeSimone, A., Tatone, A., 2012. Crawling motility through the analysis of model locomotors: two case studies. *Eur. Phys. J. E* 35, 85. (doi: 10.1140/epje/i2012-12085-x)
- [5] DeSimone, A., Guarnieri, F., Noselli, G., Tatone, A., 2013. Crawlers in viscous environments: linear vs non-linear rheology. *Int. J. Non-Linear Mech.* 56, 142-147. (doi: 10.1016/j.ijnonlinmec.2013.02.007)
- [6] DeSimone, A., Gidoni, P., Noselli, G., 2015. Liquid Crystal Elastomer Strips as Soft Crawlers. *J. Mech. Phys. Solids* 85, 254–272. (doi: 10.1016/j.jmps.2015.07.017)
- [7] Gidoni, P., Noselli, G., DeSimone, A., 2014. Crawling on directional surfaces. *Int. J. Non-Linear Mech.* 61, 65-73. (doi: 10.1016/j.ijnonlinmec.2014.01.012)
- [8] Hirose, S., 1993. *Biologically Inspired Robots: Snake-Like Locomotors and Manipulators*. Oxford University Press, Oxford.
- [9] Ikuta, K., Hasegawa, T., and Daifu, S. 2003. Hyper redundant miniature manipulator Hyper Finger for remote minimally invasive surgery in deep area. In *Proceeding of IEEE International Conference on Robotics and Automation*, Vol. 1, Taipei, pp. 1098–1102. (doi: 10.1109/ROBOT.2003.1241739)
- [10] Magnasco, M.O. 1993. Forced thermal ratchets. *Phys. Rev. Lett.* 71:1477-1481. (doi: 10.1103/PhysRevLett.71.1477)
- [11] Menciassi, A. and Dario, P. 2003. Bio-inspired solutions for locomotion in the gastrointestinal tract: background and perspectives. *Phil.Trans. R. Soc. Lond. A* 361:2287–2298. (doi: 10.1098/rsta.2003.1255)
- [12] Menciassi, A., Accoto, D., Gorini, S., Dario, P., 2006. Development of a biomimetic miniature robotic crawler. *Auton. Robot* 21, 155-163. (doi: 10.1007/s10514-006-7846-9)

- [13] Mielke, A., Theil, F., 2004. On rate-independent hysteresis models. *NoDEA: Nonlinear Differential Equations and Applications*, 11(2), 151–189. (doi: 10.1007/s00030-003-1052-7)
- [14] Mielke, A., 2005. Evolution of rate-independent systems. In C. Dafermos and E. Feireisl, editors, *Handbook of Differential Equations, evolutionary equations*, Elsevier.
- [15] Mielke, A., Roubíček, T., 2015. *Rate-Independent Systems. Theory and Application*. Springer, Berlin.
- [16] Montino, A., DeSimone, A., 2015. Three-sphere low-Reynolds-number swimmer with a passive elastic arm. *Eur. Phys. J. E* 38:42. (doi: 10.1140/epje/i2015-15042-3)
- [17] Noselli, G., DeSimone, A., Tatone, A., 2013. Discrete one-dimensional crawlers on viscous substrates: achievable net displacements and their energy cost. *Mech. Res. Commun.* 58, 73–81. (doi: 10.1016/j.mechrescom.2013.10.023)
- [18] Noselli, G., DeSimone, A., 2014. A robotic crawler exploiting directional frictional interactions: experiments, numerics, and derivation of a reduced model. *Proc. Roy. Soc. London A* 470, 20140333. (doi: 0.1098/rspa.2014.0333)
- [19] Recho, P., Truskinovsky, L., 2016. Maximum velocity of self-propulsion for an active segment, *Mathematics and Mechanics of Solids* 21, 263–278. (doi: 10.1177/1081286515588675)
- [20] Sheshka, R., Recho, P., Truskinovsky, L. 2015. Pseudo energy wells in active systems. Preprint ArXiv 1509.02753v1.
- [21] Steigenberger, J., Behn, C., 2012. *Worm-Like Locomotion Systems. An intermediate theoretical Approach*. Oldenbourg Wissenschaftsverlag, Berlin.
- [22] Zimmermann, K., Zeidis, I., Behn, C., 2009. *Mechanics of terrestrial locomotion*. Springer, Berlin.